INDEPENDENT COMPONENT ANALYSIS OF SINGLE-TRIAL EVENT-RELATED POTENTIALS

Tzyy-Ping Jung[1], Scott Makeig[2], Marissa Westerfield[3,4]
Jeanne Townsend[3,4], Eric Courchesne[3,4], Terrence J. Sejnowski[1,3]

[1]Howard Hughes Medical Institute and Computational Neurobiology Lab
The Salk Institute, P.O. Box 85800, San Diego, CA 92186-5800
{jung,scott,terry}@salk.edu
[2]Naval Health Research Center, P.O. Box 85122, San Diego, CA 92186-5122
[3]University of California, San Diego, CA 92093
[4]Children's Hospital Research Center, San Diego, CA 92037

ABSTRACT

Single-trials in event-related potential (ERP) experiments consists of electroencephalographic (EEG) recordings of brain activity time-locked to experimental events. These are usually averaged across a set of similar or identical events to increase their signal/noise ratio relative to non-phase locked EEG activity and non-brain artifacts, regardless of the fact that response activity may vary widely across trials in time course and scalp distribution. Averaging thus may not be suitable for investigating neuron brain dynamics involving transitory and intermittent subject cognitive states. Analysis of single ERP epochs, on the other hand, while ideal, suffers from confusions caused by significant EEG artifacts associated with blinks, eye-movements, and muscle noise, by large non-phase locked background EEG activities, and by the wide variability in latencies and amplitudes of ERP waveforms from trial to trial. This study introduces a new visualization tool, the 'ERP image', for investigating variability in latencies and amplitudes of event-evoked responses in spontaneous EEG or MEG records. Second, we apply a new linear decomposition tool, Independent Component Analysis (ICA) [1], to multichannel single-trial EEG records to derive spatial filters that decompose single-trial EEG epochs into a sum of temporally independent and spatially fixed components arising from distinct or overlapping brain or extra-brain networks. We demonstrate the power of the proposed analysis and visualization tools for single-trial ERP analysis through analysis of sample data sets from one normal and one autistic subject.

1. INTRODUCTION

Scalp-recorded *event-related potentials* (ERPs) are voltage changes in the ongoing *electroencephalogram* (EEG) that are both time- and phase-locked to a class of experimental events. These field potential records are usually averaged to increase their signal/noise ratio relative to artifacts and non-phase locked EEG activity. However, this averaging method disregards the fact that in different epochs response activity may vary widely in time course and/or scalp distribution, possibly, reflecting differences in subject expectation, attention, arousal, and task strategy [2, 3]. Analysis of single trials may potentially reveal much richer information about event-related brain dynamics, but suffers from: (1) difficulties in ignoring or removing pervasive artifacts associated with blinks, eye-movements and muscle noise which are a serious problem for EEG interpretation and analysis, especially when blinks and muscle movements occur too frequently, as in some patient groups; (2) poor signal-to-noise ratio arising from the fact that non-phase locked background EEG activities often are larger than phase-locked response components, making extraction of event-related brain dynamics difficult; (3) variability in latencies and amplitudes of both event-related responses and endogenous EEG components.

We present here two new methods for analyzing and visualizing multichannel unaveraged single-trial ERP records that solve or alleviate these problems. First, we introduce a new visualization tool, the 'ERP image' for visualizing phase, amplitude and timing relations

between event-related single-trial EEG activity time-locked to experimental events (e.g., stimulus onsets or subject responses). Next, we demonstrate decomposition of multi-channel EEG epochs using Independent Component Analysis (ICA). ICA decomposes multi-channel complex data into spatially fixed and temporally independent components whose linear mixtures form the input data records. Applied to the single-trial EEG records from subjects in a visual selective attention experiment, ICA derived components whose dynamics were related to stimulus onsets and/or subject responses in distinctly different ways. We demonstrate, through analysis of two sample data sets, the power of the proposed analysis and visualization tools for increasing the amount and quality of information about event-related brain dynamics that can be derived from single-trial EEG data.

2. INDEPENDENT COMPONENT ANALYSIS OF EEG DATA

In 1995, Bell and Sejnowski [4] proposed a simple neural network algorithm that blindly separates mixtures, x, of independent sources, s, using infomax. They showed that maximizing the joint entropy, $H(y)$, of the output of a neural processor minimizes the mutual information among the output components, $y_i = g(u_i)$, where $g(u_i)$ is an invertible bounded nonlinearity and $u = Wx$, a version of the original sources, s, identical save for scaling and permutation. Lee et al. [1] generalized the infomax algorithm to perform blind source separation on linear mixtures of sources with either sub- or super-Gaussian distributions. For details regarding the algorithms, see [1, 4].

ICA is suitable for performing blind source separation on EEG data because: (1) it is plausible that EEG data recorded at multiple scalp sensors are linear sums of temporally independent components arising from spatially fixed, distinct or overlapping brain or extra-brain networks, and, (2) spatial smearing of EEG data by volume conduction does not involve significant time delays. For details regarding ICA assumptions underlying EEG analysis, please see [5, 6]. In single-trial EEG analysis, the rows of the input matrix x are the EEG signals recorded at different electrodes, while the columns are measurements recorded at different time points. The rows of the independent output data matrix $u = Wx$ are time courses of activation of the ICA components, and the columns of the inverse matrix, W^{-1}, give the projection strengths of the respective components onto the scalp sensors. The scalp topographies of the components provide evidence as to their physiological origin (e.g., eye activity should project mainly to frontal sites). EEG signals of interest (e.g., event-related brain signals) can then be obtained by projecting selected ICA components back onto the scalp as $x' = (W)^{-1}u'$, where u' is the matrix of activation waveforms, u, with rows representing activations of 'unwanted' or 'noise' sources set to zero.

3. METHODS AND MATERIALS

EEG data were recorded at 29 scalp electrodes and 2 periocular (EOG) placements from one normal and one high-functioning adult autistic subject who participated in a 2-hr visual selected attention task in which they were instructed to attend to circles flashed in random order at one of five locations laterally arrayed 0.8 cm above a central fixation point. Locations were outlined by five evenly spaced 1.6-cm blue squares displayed on a black background at visual angles of ±2.7 deg and ±5.5 deg from fixation. Attended locations were highlighted through entire 90-sec experimental blocks. Subjects were instructed to maintain fixation on the central cross and press a button each time they saw a circle in the attended location (see [9] for details). EEG data were referred to the right mastoid; data were sampled at 512 Hz.

3.1. ERP image

We have developed a new visualization tool, the ERP image for investigating variability in the latencies and amplitudes of event-related responses. To form an ERP image, potentials recorded at one channel or the activations of one ICA component are plotted as parallel colored lines and sorted in order of a relevant response measure (e.g., subject response time). The single-trials may be colored separately, or first smoothed with a narrow (e.g., 5-30 trial) moving window to increase the visibility of consistently time- or phase-locked features.

4. RESULTS

The ICA algorithm was applied separately to concatenated 31-channel single-trial EEG records from each subject. The derived independent components had a variety of distinct relations to task events. Some were clearly time- and phase-locked to stimuli presentations, while others were time- and phase-locked to subject responses. Still others captured one category of spontaneous EEG activity, such as blinks, eye-movements, or muscle artifacts, or else a type of oscillatory or other background EEG phenomena.
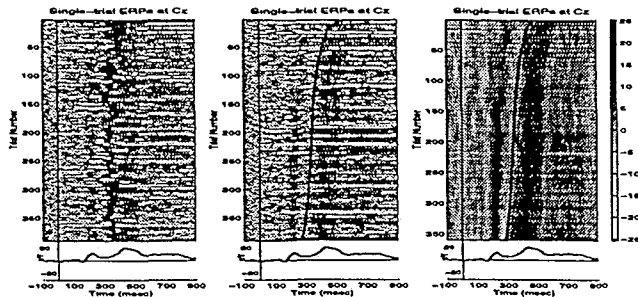
Figure 1: Example ERP images of single-trial EEG data. *(left panel)* Single-trial ERPs recorded at a central electrode (Cz) and time-locked to onsets of visual target stimuli *(thin vertical line)* with superimposed subject response times *(thick black line)*. *(middle panel)* The same 390 single trials, sorted (bottom to top) in order of increasing reaction time. *(right panel)*. To increase signal-to-noise ratio and minimize the influence of EEG activity not consistently time- and phase-locked to the experimental events, the sorted trials were averaged using a 30-trial moving window which was advanced through the data in one-trial steps.

4.1. ERP image

ERP images can be used to visualize variability in the latencies and amplitudes of event-evoked responses either in spontaneous EEG epochs themselves or in the single-trial activations of independent components of the data. An example, shown in Figure 1 *(left panel)*, plots 390 single-trial ERP epochs recorded at a central electrode (Cz) and time-locked to onsets of target stimuli *(left vertical line)*. Each colored horizontal trace represents a 1-sec single-trial ERP record whose potential variations are color coded *(color bar on right)*. The jagged thick vertical line plots subject response time in each trial. Note the trial-to-trial fluctuations in ERP latency and reaction time. The ERP average of these trials is plotted below the ERP image. Next, the same single trials were sorted in order of increasing subject response time (RT) and plotted both before *(middle panel)* and after *(right panel)* smoothing with a 30-trial rectangular moving average. Note *(right panel)* that in all but the longest-RT trials the early positive feature (P2) is time-locked to stimulus onset (i.e. it is stimulus-locked), while in relatively long-RT trials, the P2 is absent or later and weaker. Also, the later P3 feature follows the response by about 100 ms in nearly all trials (i.e., it is response-locked). ERP-image plots allow easy visualization of relations between event-related EEG trials and single-trial contributions to the ERP average. ERP images make visible links between amplitudes and

latencies of individual event-related responses and subject behavior. They also reveal several problems of conventional response averaging.

First, the trial-to-trial invariance of ERP signals cannot be assumed. In fact, not every trial in these data has a response morphology that resembles the averaged ERP waveform *(bottom traces)*. Second, ERP components systematically associated with subject response latency are temporally smeared in the stimulus-locked average *(bottom traces)* (e.g., the P3 feature in the time period 300 to 900 ms), often making the averaged ERP a relatively poor representative of the underlying event-related response processes.

4.2. Removing blink and eye-movement artifacts from EEG records

In visual experiments, autistic subjects may tend to blink more frequently than normal subjects [7]. ICA, applied to a data set from an autistic subject in which about 50% of the trials were contaminated by blinks, successfully isolated blink artifacts to a single component (Fig. 2A, *left*) whose contributions could be removed from the EEG records by subtracting out the component projection from the data [8]. Though the subject was instructed to fixate during each 90-sec block, the technician noticed that his eyes tended to drift towards target stimuli presented at peripheral locations. A second ICA component accounted for these horizontal eye-movements (Fig. 2A, *right*). Fig. 2A *(lower right)* shows separate ERP averages (at periocular site EOG2) of responses to targets presented at the five different attended locations. The maximum activation of the prominent eye movement-related component scaled near linearly with the angle of the stimulus location from fixation. Its scalp pattern was also consistent with a pattern expected for lateral eye movements. Note the difference in scalp topography between the two components accounting for blinks and eye movements (Fig. 2A).

Figure 2B *(left)* shows 641 single-trial EEG epochs recorded at one frontal electrode (EOG2), *(middle)* the signals identified as blink and eye-movement artifacts by ICA, and *(right)* the corrected EEG trials obtained by subtracting both artifacts from the original records. As can be seen, a large number of blink and eye-movement artifacts *(center panel, blue and red lines)* were removed from the records by this procedure.

Figure 2C shows the averaged ERPs at electrode EOG2 in response to stimuli presented at the five different attended locations, before and after artifact-removal *(blue and red traces, respectively)*. After artifact correction, the averaged ERP responses to stimuli presented at the five different locations did not depend on

stimulus location.

Figure 2D shows the same artifact-removal procedure applied to data collected from a normal subject. After artifact correction, the ERPs at site EOG2 for the five different target locations were quite similar and showed strong inferior frontal activity identified as P3f by Makeig et al. [9], a newly identified subcomponent of the P300 or Late Positive Complex of the visual target ERP. Rejection of the contaminated EEG epochs could not wholly avoid these artifacts since their amplitudes were often smaller than typical or practical rejection thresholds for rejecting blinks and eye-movements. If, alternatively, the periocular data channels (here, EOG1 and EOG2) had been used as references to regress out contributions to signals at adjacent sites [10, 11], cerebral activity expressed in those channels would have been subtracted from every scalp site, and the reference sites themselves would have become silent. This may explain the failure of previous ERP literature to identify the P3f component.

4.3. Extracting event-related brain activity from EEG Records

As mentioned previously, a second problem of single-trial analysis concerns the extraction of single-trial ERPs from background EEG processes that are not both time- and phase-locked to the stimulus. ICA, applied separately to each data set, separated stimulus-locked, response-locked, and non-phase locked background EEG activities into different independent components. Numbers of components in each class varied across subjects. Figure 3A shows the summed projections of the subgroups of ICA components accounting primarily for (*left*) stimulus-locked, (*middle*) response-locked, and (*right*) remaining non-phase locked background EEG activity at site PO3. Notice that, (1) both the response latencies and active durations of the early stimulus-locked P1 and N1 components were stable in nearly all trials; (2) the peak of the later P3 component covaried with response time, and was weak in longest-RT trials; and, (3) the projections of ICA components accounting for non-phase locked background EEG activity contributed very little to the averaged ERP (*right panel, bottom trace*). These results indicate that ICA makes possible the extraction and separation of event-related brain phenomena of all types from spontaneous single-trial EEG records.

4.4. Realigning single-trial ERPs

Figure 3B (*left panel*) shows the raw artifact-corrected single-trial ERP epochs (the sum of the data shown in Fig. 3A) at left posterior site PO3. Response latency
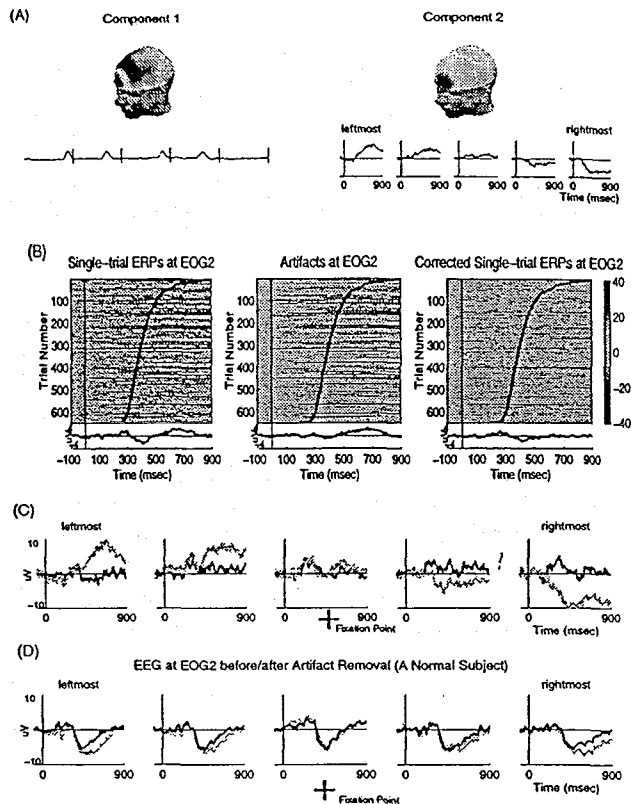

Figure 2: (A) (*left*) Scalp topography and 5 consecutive 1-sec epochs of the activation time course of an ICA component counting for blink artifacts in 641 single trials recorded from an adult autistic subject. (*right*) The approximate scalp topography of an "eye-movement" component and its *averaged* activation time courses in response to target stimuli presented at five different locations. (B) (*left*) ERP images of single-trial ERPs at site EOG2 time locked to targets presented at all five attended locations, sorted by subject response time; (*center*) projections of components identified as artifacts by ICA; (*right*) corrected single-trial ERPs obtained by subtracting the ICA-extracted artifacts from the original data. (C) Averaged ERPs at site EOG2 to targets presented at the respective five attended locations, before (*faint traces*) and after (*bold traces*) artifact removal. Removing eye drift artifacts from the single-trial ERPs revealed the apparent independence of the small visual response from stimulus location. (D) The same artifact-removal procedure applied to the EEG data collected from a normal subject. Note that, the difference in the target ERPs before/after artifact removal are progressively larger in responses to stimuli presented farther from the central fixation point, consistent with an involuntary tendency of both subjects to move their eyes towards presented targets.

(A) Stimulus-locked Activity at PO3 — Response-locked Activity at PO3 — Background Activity at PO3

(B) Single-trial ERPs at PO3 — Response-aligned ERPs — ICA-aligned ERPs

(C) P3 Activity at PO3 (All Trials) — P3 Activity in 'Good' Trials — P3 Activity in 'Bad' Trials
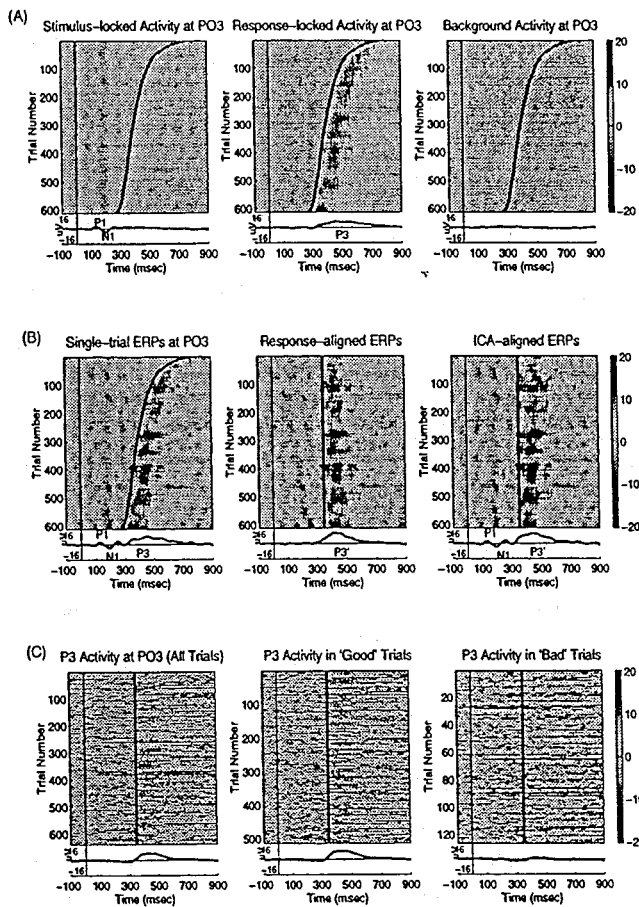
Figure 3: (A) Projections of ICA components at a posterior scalp site (PO3) accounting for, respectively, stimulus-locked (*left*), response-locked (*middle*), and non-phase locked or background (*right*) EEG activity. (B) Artifact-corrected single-trial ERP records time-locked, respectively, to stimulus onsets (*left*), and subject responses (*center*). Note that the early ERP features (P1, N1, etc.) are not in phase in the response-locked trials (*center*) and do not appear in the response-locked average (*center bottom*). Projections of the response-locked components were aligned to median reaction time (355 ms) and summed with stimulus-aligned component projections (*right*), forming an enhanced stimulus-aligned ERP (*right bottom*). (C.) Projections of the ICA components accounting for response-locked P3 activity (*left*) could be segregated into 'good-P3' trials (*center*), whose waveforms resembled the averaged P3, and 'bad-P3' trials (*right*) whose average was very different from those of the good trials or of all the trials (*bottom right*). To reveal inter-trial difference, in (C) the ERP images are unsmoothed.

differences produce a pronounced temporal smearing of the P3 feature in the averaged ERP (*bottom left*). Realigning the single-trial ERP epochs to the median reaction time (*center panel*) sharpens the averaged P3 , but unfortunately makes the early stimulus-locked activity out of phase and smears out the early ERP features (100-300 ms). However, because ICA separated stimulus-locked and response-locked activity into different independent components, we could realign the time courses of the response-locked P3 component to the median reaction time and project the adjusted data, along with the unaligned time courses of stimulus-locked early components (P1, N1, etc.), back onto the scalp sensors (*right panel*). This realignment preserves the early stimulus-locked responses (P1/N1) while sharpening the response-locked P3, minimizing temporal smearing in the averaged ERP arising from performance fluctuations (compare *left* and *right* panels).

4.5. Classifying Sub-types of endogenous ERPs

The P3 (or P300) component in response to expected but unpredictable target stimuli typically peaks 300 ms or more after onsets of infrequently presented target stimuli. However, P3 amplitude and waveshape may vary widely from trial to trial, possibly because subjects may employ different strategies for performing the task, even within the same session. Several studies [3, 12] have reported a number of different single-trial response subtypes. However, classifying subtypes of single-trial scalp ERPs remains difficult because the presence of large artifacts and non-task related background EEG activity in the single-trials. Because ICA can separate event-related responses from the background EEG and EEG artifacts, it allows us to examine the subtypes of each event-related response by classifying the relatively 'clean' spatiotemporal P3 feature extracted by ICA for each trial. This can simply be done by first realigning the time courses of the response-locked P3 component(s) to the median response time, then projecting only those aligned activations back to scalp sensors (Fig. 3C, *left panel*). By using the averaged 'realigned' P3 waveform (*bottom trace, left panel*) as a template for correlating with the waveform of each single-trial activation (*left panel*), relatively 'good' and 'bad' P3 trials can then be identified. For example, Fig. 3C (*center*) shows the ERP image plots of 'good-P3' trials, in which the P3-component activation resembles the averaged activation ($r \geq 0.3$, ~80% of the trials) and remaining 'bad-P3' trials (*right*) in which the response morphology of the P3-component activation differs sharply ($r < 0.3$) from the activation average.

5. CONCLUSIONS

We have developed analytic and visualization tools for analysis of multichannel single-trial EEG records. ERP images make visible systematic relations between single-trial EEG records, experimental events, and the respective ERP averages. ERP images can also be used to display relationships between phase, amplitude and timing of event-related EEG components that are time-locked either to stimulus onsets, to subject responses, or to other events. Single-trial ERP analysis based on Independent Component Analysis allows blind separation of multichannel complex EEG data into a sum of temporally independent and spatially fixed components. Our results show that ICA can separate artifactual, stimulus-locked, response-locked, and non-event related background EEG activities into separate components, allowing (1) removal of pervasive artifacts of all types from single-trial EEG records, and (2) identification and segregation of stimulus- and response-locked EEG components, (3) realignment of the time courses of response-locked components to prevent temporal smearing in the average, which in these experiments is mostly time-locked to fluctuations in response time, and (4) classification of response subtypes.

The analysis and visualization tools proposed in this study increase the amount and quality of information on event- or response-related brain signals that can be extracted from ERP data, and appear broadly applicable to electrophyiological research on normal and clinical populations.

6. REFERENCES

[1] T.W. Lee, M. Girolami and T.J. Sejnowski (submitted) Independent component analysis using an extended infomax algorithm for mixed sub-Gaussian and super-Gaussian sources. *Neural Computation*.

[2] H. Yabe, F. Satio & Y. Fukushima (1993) Median method for detecting endogenous event-related brain potentials, *Electroencephalog. clin. Neurophysiolog.* 87(6):403-7.

[3] A.R. Haig, E. Gordon, G. Rogers & J. Anderson (1995) Classification of single-trial ERP sub-types: Application of globally optimal vector quantization using simulated annealing, *Electroencephalog. clin. Neurophysiolog.* 94(4):288-97.

[4] A.J. Bell & T.J. Sejnowski (1995). An information-maximization approach to blind separation and blind deconvolution, *Neural Computation* 7:1129-1159.

[5] S. Makeig, T-P Jung, D. Ghahremani & T.J. Sejnowski (1996). *Independent component analysis of simulated ERP data*, Tech. Rep. INC-9606, Institute for Neural Computation, San Diego, CA.

[6] S. Makeig, T-P Jung, A.J. Bell, D. Ghahremani, and T.J. Sejnowski (1997) Blind separation of event-related brain responses into independent components, *Proc. Natl. Acad. Sci. USA*, USA, 94:10979-84.

[7] J.G. Small (1971) Sensory evoked responses of autistic children, In: *Infantile Autism*, 224-39.

[8] T-P Jung, C. Humphries, T.W. Lee, S. Makeig, M.J. McKeown, V. Iragui, T.J. Sejnowski (1998) Extended ICA removes artifacts from electroencephalographic Data, In: *Advances in Neural Information Processing Systems* 10, 894-900.

[9] S. Makeig, M. Westerfield, J. Covington, T-P Jung, J. Townsend, T.J. Sejnowski, and E. Courchesne (submitted) Independent components of the late positive response complex in a visual spatial attention task," *J. Neuroscience*.

[10] S.A. Hillyard and R. Galambos (1970). Eye-movement artifact in the CNV, *Electroencephalog. clin. Neurophysiolog.*, 28(2): 173-182.

[11] J.C. Woestenburg, M.N. Verbaten, and J.L. Slangen (1983) The removal of the eye-movement artifact from the EEG by regression analysis in the frequency domain, *Biological Psychology* 16:127-47.

[12] S. Suwazono, H. Shibasaki, S. Nishida, M. Nakamura, M. Honda, T. Nagamine, A. Ikeda, J. Ito & J. Kimura (1994) Automatic detection of P300 in single sweep records of auditory event-related potential, *J. Clin. Neurophysiolog.* 11(4):448-60.